Investigation of a New Readout Scheme for High Resolution Scintillation Crystal Arrays Using Photodiodes

Craig S. Levin, *Member, IEEE*, and Edward J. Hoffman, *Senior Member, IEEE*

Division of Nuclear Medicine and Biophysics, UCLA School of Medicine
Los Angeles CA 90095-6948

Abstract

We are exploring the possibility of using PIN photodiodes to readout the scintillation crystals used in Positron Emission Tomography (PET) detector designs. Semiconductor photodetectors typically have a lower signal to noise ratio than photomultiplier tubes (PMTs). However, they have the advantage of compactness, and, thus, scintillation crystal readout schemes not available to PMTs because of their size and geometry limitations, are readily available to photodiodes. With current PET detector designs, only a small fraction of the available scintillation light, created from 511 keV gamma ray interactions within the crystal, is collected. Scintillation light collection studies were performed for several crystal geometries and surface treatments using both simulations and measurements. In this report, we present a feasible photodiode readout scheme that allows greater than 90% of the available scintillation light created in either BGO or LSO scintillation crystals to be collected by the photodetector. This improvement in light collection with the photodiode readout somewhat compensates for its lower inherent signal to noise ratios and makes it feasible for use in PET detectors. A coincident timing spectrum resolution of 9.4 ns FWHM was measured for 511 keV interactions with one LSO crystal coupled to a photodiode, the other to a PMT.

I. INTRODUCTION

In current Nuclear Medicine scintillation camera instrumentation, photomultiplier tubes (PMT) are used for scintillation light readout. These devices have the advantages of high gain and signal-noise-ratios (SNR). However, disadvantages of the PMT are the bulkiness and the cost. In most Positron Emission Tomography (PET) detector designs described in the literature, arrays of long and narrow discrete or pseudo-discrete BGO or LSO scintillation crystals are coupled either one to one [1-3] or to four PMTs [4-6], respectively. Various reflectors and surface treatments are used to channel the light towards the small end faces of the crystals where the light is readout. The fraction of the available scintillation light collected from a 511 keV interaction within a given crystal generally decreases as the ratio of the crystal length to cross-sectional area increases. This dependence is due to the larger number of surface interactions (reflections/refractions) encountered by scintillation photons within longer and narrower crystals. In addition, if the side faces of these long and thin crystals are not highly polished, there is less chance that a scintillation photon will undergo total internal reflection, further diminishing the light yield. The result is that in current PET detector designs, only a small fraction of the scintillation light available from 511 keV interactions within the crystal is collected. Ideally, it would be best to readout long, narrow scintillation crystals from all sides or at least from the largest faces. In this case the optical photons would undergo a smaller number of reflections before exiting the crystal. However, for compact scintillation crystal arrays, this ideal readout is impossible with PMTs, because of their size and geometry.

Semiconductor photodetectors, such as silicon PIN photodiodes (PDs) have the advantage of compactness. Scintillation crystal readout schemes not available to PMTs because of their bulkiness, are readily available to PDs. For example, the side faces of long and narrow crystals in an array can be readout using PDs, provided the PDs are thin enough to insert in between crystal planes without an unusual increase in dead area. PDs have other advantages over PMTs such as higher quantum efficiency and lower cost. However, as devices, PDs have a lower SNR than photomultiplier tubes (PMTs) due to capacitive noise and dark current. Others [7-17] have proposed using arrays of PDs and avalanche photodiodes (APDs) to readout crystal arrays in PET. These efforts mainly concentrated on reading out arrays of long and narrow scintillation crystals end-on. Scintillation light collection studies were performed for several crystal geometries and surface treatments using both simulations and measurements. In this report, we present a feasible scintillation crystal room temperature photodiode readout scheme that allows greater than 90% of the available scintillation light created in either BGO or LSO to be collected by the photodetector. This improvement in light collection with the photodiode readout somewhat compensates for its lower inherent SNR and makes it feasible for use in PET. We demonstrate that the proposed scheme has sufficient SNR to meet the requirements of PET.

II. METHODS

A. *Potential Photodiode Readout Scheme*

Figure 1 depicts a potential photodiode readout scheme for scintillation crystal arrays used in PET. Readout of the side face of a long and narrow crystal has the advantage of collecting a larger fraction of the scintillation light created in a crystal by a 511 keV gamma ray interaction compared to the standard end face readout. Thin (<250μm) 1-D arrays of room temperature PD strips could accomplish this side readout. These PD arrays could easily fit in between crystal planes without introducing additional dead area to that already present in current designs which have ~250-400μm of white reflector material between crystals. The PD cannot be made too thin since this would cause large device capacitance, and,, therefore, higher noise. The photodiodes would be readout with an ASIC array of miniature low noise charge sensitive preamplifiers built directly under the array. The side readout scheme depicted in the figure would be unavailable to PMT designs.

0018-9499/97$10.00

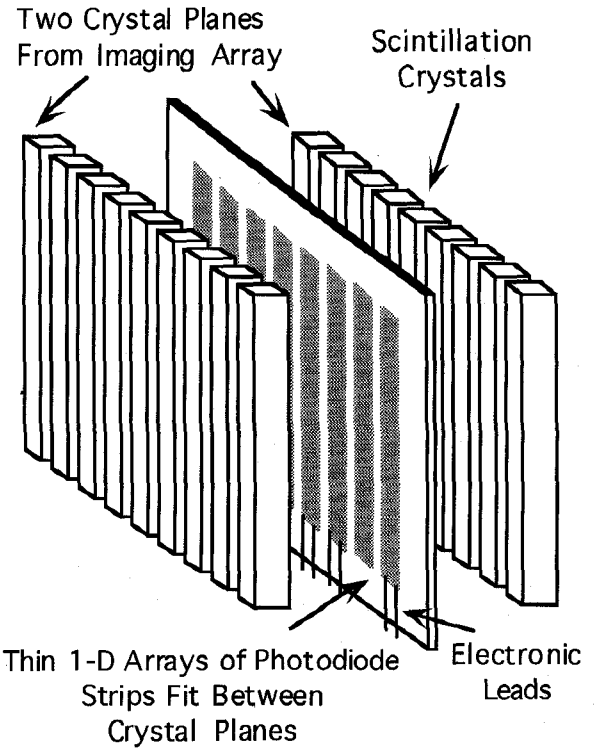

Figure 1. Schematic of a potential photodiode readout of a scintillation crystal array (only two crystal planes shown). The thickness of 1-D array of photodiode strips can be made < 250μm to minimize the dead area between crystal planes.

B. Monte Carlo Simulations

Optical photon tracking Monte Carlo simulations were performed with DETECT [18] to determine light output characteristics of BGO and LSO scintillation crystals for various readout conditions. We assume that a gamma ray interaction will create a point source of light. A 2x2 mm^3 (high resolution) cross-sectional crystal area was used for these studies. We use a diffuse, 98% reflective surface on the crystal faces not connected to the photodetector. We are interested only in relative light collection values so the value of the photodetector quantum efficiency used was not crucial for these studies. The average fraction of available scintillation light collected for side vs. end face readout of a scintillation crystal was determined as a function of its length. We determine this average by weighting the calculated fraction of collected light for a given interaction point within a crystal with the gamma ray interaction probability at that location. The 511 keV absorption lengths used for LSO and BGO are 11.3 and 10.6 mm, respectively. The study was performed for both ground as well as polished crystal faces. We do this because in practice it is not always possible to have highly polished crystal faces. Ground side faces will further diminish the fraction of the available scintillation light collected when using readout of the end face of a crystal. This decrease will be magnified for longer and narrower crystals.

C. Experimental Measurements

To demonstrate that the PD readout scheme has sufficient SNR for PET, energy spectra measurements were performed with both a PD and a PMT, for comparison. The PD was a Hamamatsu S3588 (3 x 30 mm^2 active area). Typical dark current specifications of this PD range from 3-10 nA at room temperature. A ^{22}Na (511 keV) gamma ray source was used for the measurements. Two sizes of LSO crystals (2x2x10mm^3 and 2.5x2.5x20mm^3, both highly polished on all sides; the smaller crystal came from slightly better quality LSO) and four sizes of BGO crystals (1.5x1.5x10mm^3, sides and one end ground, the other end "pseudo-polished"; 2x2x10mm^3, sides and ends polished; 2x2x20mm^3, sides and ends "pseudo-polished"; 2x2x30mm^3, sides and ends "pseudo-polished") were used, each coupled via optical grease to the PD. The sides of the crystals not in contact with the PD were wrapped in white Teflon as a reflector. The PD was biased with 70 V, readout with an ORTEC 142A charge sensitive preamplifier (energy output), and amplified and shaped with a CANBERRA 2021 (shaping time: 250 ns and 1.0 μs for LSO and BGO, respectively). The PMT anode signal (energy) was read out with an ORTEC 9301 fast preamplifier and the same spectroscopy amplifier and shaping parameters were used. The trigger for the ADC (CAMAC BiRa Transient Digitizers) was created from a gate (ORTEC 416A) generated by a timing single channel analyzer unit (CANBERRA 2035A). Data acquisition was controlled by LabView (National Instruments) on a Macintosh IIfx through a GPIB control interface to the CAMAC crate. Measured results were compared to those obtained by simulations.

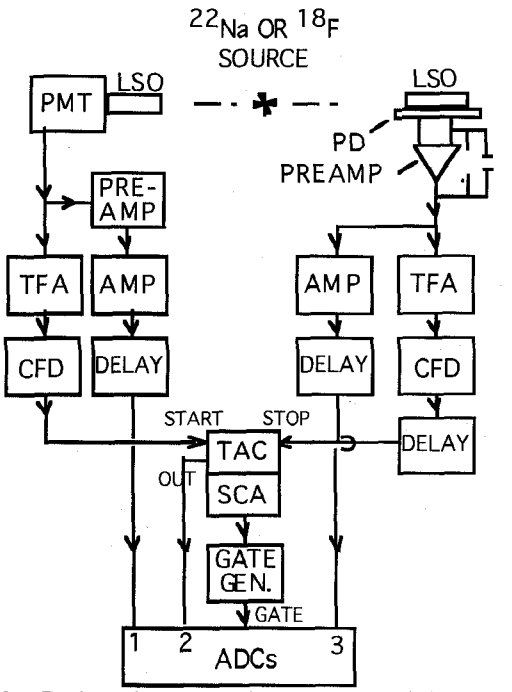

Figure 2. Basic pulse processing circuit used for coincidence timing resolution measurements. Start: LSO/PMT; Stop: LSO/PD.

Coincidence timing spectra were measured using the set-up shown in Figure 2. Both ^{22}Na and ^{18}F were used as a source of back-to-back annihilation gamma rays. A 2.5x2.5x20mm^3 LSO crystal was coupled side-on to the PD and a 4x4x10mm^3 LSO crystal was coupled end-on to an RCA C31024 PMT. Again the ORTEC 142A (with energy and timing outputs) read out the PD. The timing output signal from the ORTEC 142A and the 10th dynode signal from the PMT channel were amplified with the ORTEC 579 Fast

Timing Filter Amplifiers (zero integration and differentiation for both channels). The timing was picked-off from each amplified timing pulse with an ORTEC 935 Quad Constant Fraction Discriminator (CFD). The PMT 10th dynode channel served as a start for the TENELEC TC863 Time to Amplitude Converter / Single Channel Analyzer (TAC/SCA) and the PD timing channel provided the stop. The SCA portion of the TC863 was fed into a gate and delay generator, which provided the trigger for the digitizers. A delay (ORTEC 425) positioned the timing spectra on the digitized TAC value axis and enabled a time calibration. For simultaneous measurements of detector energies that contribute to the timing spectra, the PD and PMT energy signals were amplified and shaped with the CANBERRA 2021 and ORTEC 673 spectroscopy amplifiers, respectively (250ns shaping time). To understand how the PD noise will contribute to the timing resolution measured, the CFD threshold was set to zero for both channels and the TAC, and energy signals from the PD and PMT channels were digitized and the values saved in list mode for each event.

III. RESULTS

A. Simulations

Table 1 summarizes the results from the Monte Carlo simulations of light collected. Light collected in 2x2x10 mm^3, 2x2x20 mm^3, and 2x2x30 mm^3 crystals was studied with both end face (2x2 mm^2 area) and side face (2x10 mm^2 area, 2x20 mm^2 area, and 2x30 mm^2 area) readout of the scintillation light. For each case, both perfectly polished and highly ground surface treatment results are shown. In reality, it may only be possible to achieve surfaces somewhere between these idealized treatments. The values in the table are the average fraction (%) of the total available light collected. The average was calculated over several origins of the source of light (depths of interaction) within a crystal by weighting the location of the origin with the interaction probability at that location.

Table 1. Comparison of light collected for side and end readout schemes for 3 sizes and 2 surface treatments of LSO and BGO crystals. Values shown are % of available light collected.

Readout/ Surfaces	2x2x10 mm^3		2x2x20 mm^3		2x2x30 mm^3	
	LSO	BGO	LSO	BGO	LSO	BGO
End/ Polished	61.9	63.8	55.3	53.1	50.0	44.6
Side/ Polished	89.9	87.1	90.6	88.9	91.4	88.3
End/ Ground	58.5	49.8	37.7	31.1	23.9	19.1
Side/ Ground	86.7	83.2	88.3	83.0	89.0	83.3

In Table 1, we see that the light collection fraction is relatively insensitive to crystal length and surface treatment with side readout. In addition, for a series of simulations performed with narrower (< 2mm wide) crystals and side readout, the light collected was fairly independent of crystal width. Thus, side readout opens the possibility of reducing the width of the crystals below 2 mm (and, thus, improving intrinsic resolution) while still collecting a high fraction of the available scintillation light. Using end readout, however, the predicted light collection strongly depends on the crystal length, width and surfaces.

From the table we also see the clear improvement in the amount of scintillation light collected for side compared to end readout. The improvement is huge when the crystal is ground ("lossy") and significant even when the crystal surface is perfectly specular. The improvement is also greater for longer crystals, due to the larger number of reflections photons undergo before exiting a crystal end compared to side face. For perfectly polished crystals (the ideal case), the predicted improvement of side over end readout of the scintillation light is roughly 45, 64 and 83% for the 2x2x10mm^3 , 2x2x20mm^3, 2x2x30mm^3 size LSO crystals, respectively, and 37, 67 and 98 % for the 2x2x10mm^3, 2x2x20mm^3, 2x2x30mm^3 size BGO crystals, respectively. For narrower (<2mm) crystal widths simulated, these differences were larger.

The large advantage of side over end readout becomes most evident for less polished crystals. For 2x2x10mm^3, 2x2x20mm^3, and the 2x2x30mm^3 size ground crystals, the predicted improvement in light collected for side over end readout is, respectively, 48, 120 and 272% for LSO, and 67, 167, and 336% for BGO. These results are important since in reality it is not easy to obtain a large quantity of perfectly polished crystals and the difference in light collected between the two surface treatments is not significant for side readout of the scintillation light. For all crystal lengths and widths studied, with side readout, the fraction of available light collected was greater than 88% (83%) for highly polished (ground) crystal surfaces. In practice, this side readout scheme of a scintillation crystal array can only be realized with the compactness of a thin semiconductor photodetector.

B. Measurements

To demonstrate that the PD readout scheme proposed has sufficient SNR for PET, the important comparison to make is between energy measurements performed with scintillation crystals readout from the side face with a PD and from the end face with a PMT. Figure 3 shows this comparison for the 2x2x10mm^3 and 2.5x2.5x20mm^3 sizes of LSO crystals (large graphs), and for the 1.5x1.5x10mm^3, 2x2x10mm^3, 2x2x20mm^3, and 2x2x30mm^3 sizes of BGO (small graphs). The spectroscopy amplifier gain used for the PMT data was approximately twice that used for the PD. To facilitate comparisons, all PD spectra presented have the same gain and ADC channel scale on the plots. The same is true for all PMT spectra. The measured energy resolution of the 511 keV photopeak from ^{22}Na was 24% FWHM for both the PD side and PMT end readout using the 2x2x10mm^3 LSO crystal. For the 2.5x2.5x20mm^3 LSO crystal, the corresponding values were 23% for the PD and 21% for the PMT. So even though the PMT gain is higher and the noise current is lower than for the PD, with PMT end face readout of the crystal there is no significant signal to noise ratio gain over the PD side face readout for these narrow LSO crystals. This is the case since only a small fraction of the available scintillation light is collected with end readout.

In addition, as predicted by the simulations, the PD results for pulse height (photopeak position) and energy resolution (photopeak width) are fairly insensitive to the length and width of the crystal. However, because of the higher noise shoulder of the PD seen in Figure 3, the lower energy scatter continuum is not resolved ("in the noise"). We have measured the 511 keV photopeak energy resolution for

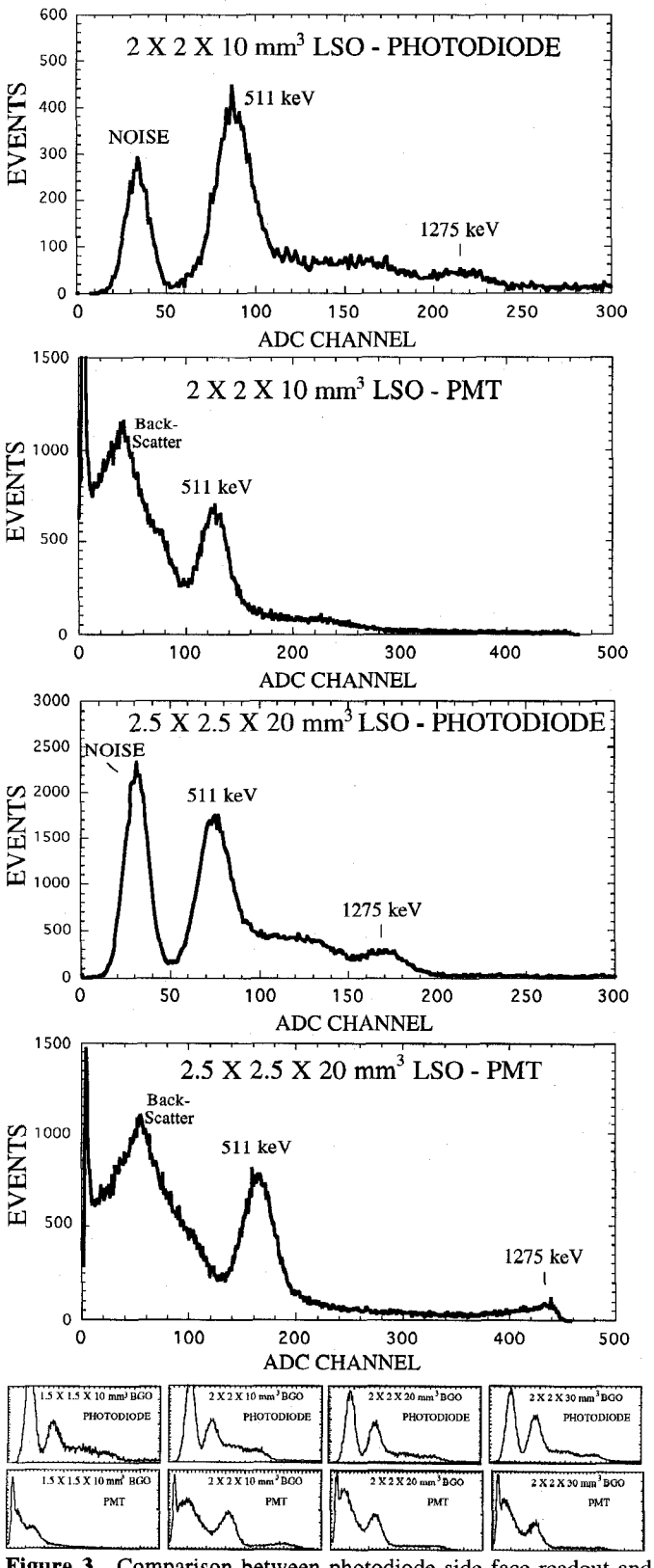

Figure 3. Comparison between photodiode side face readout and PMT end face readout, for long and narrow LSO (top large plots) and BGO (bottom small plots) crystals. ^{22}Na was used for the measurements. For the PMT spectra, the pulse height and energy resolution degrade as crystal length increases, the width decreases and for less polished surfaces. For the PD side readout spectra, light collection properties are relatively insensitive to these crystal parameters. See text for energy resolution values.

larger LSO crystals with a much higher width to length ratio and obtained much better results. For a 4x4x10 mm^3 LSO crystal, for example, we obtained 14% FWHM at 511 keV.

We also note that the sensitive area of the PD (3x3x30 mm^3) used for the spectral measurements in Figure 3 was much larger than required to read out either the 2x2x10 or 2.5x2.5x20 mm^3 LSO samples from the side. With a smaller area PD, the noise current would be reduced, and the energy resolution measurements would improve.

Using an ^{241}Am source (59.5 keV x-rays) and the average energy required to produce an electron-hole pair in silicon (3.62 eV) we calibrated the number of photoelectrons/ADC channel produced from direct x-ray interactions in the PD. From this calibration we estimate that we are producing on average approximately 6800 photoelectrons (with spread of 23% FWHM or 670e RMS) from 511 keV interactions in the 2.5x2.5x20 mm^3 LSO scintillator coupled sideways to the PD. If we assume a PD quantum efficiency for 420 nm LSO light of 50%, this implies that we are collecting roughly 13600 (1300 RMS deviation) scintillation photons at the PD. Recent measurements of absolute light yield from LSO [19] obtained 27300 ± 1400 photons/MeV which implies 14000 ± 700 photons from 511 keV interactions in LSO. Thus, we estimate that we are collecting on average roughly 97 % of the scintillation photons available from 511 keV interactions in LSO for this 2.5x2.5x20 mm^3 LSO crystal. This result is slightly higher than that seen in Table 1 which was calculated for 2 mm width crystals.

The BGO spectra plotted on a smaller scale on the bottom of Figure 3 show the PD measured results on top and that for the PMT underneath for easy comparison. The corresponding crystal sizes are, from left to right, 1.5x1.5x10mm^3, 2x2x10mm^3, 2x2x20mm^3, and 2x2x30mm^3, and the respective energy resolutions at 511 keV are 33, 30, 33, and 30 % FWHM for the side PD readout and 70, 35, 42, and 45 % for the BGO end readout. The surface conditions of each crystal were described in Section IIc. In all BGO cases, the energy resolution is superior for the PD side readout combination. This fact is especially seen for the 1.5 mm wide ground crystals, where one can barely resolve the photopeak measured with a PMT from the end. On the other hand, as predicted from the simulations, the pulse height and energy resolution are fairly insensitive to both crystal length, width and surface treatment for side readout.

Because we have the 2x2x10mm^3, 2x2x20mm^3, and 2x2x30mm^3 crystal sizes of BGO, we can directly compare simulation results of Table 1 with measurements. Figure 4 (top) shows two ^{22}Na spectra measured with the 20 and 30 mm long BGO crystals for side and end readout with a PMT. There is a clear improvement in light collection with side readout as seen by the higher photopeak position. For the 10, 20, and 30 mm lengths this improvement was measured to be 23, 26 and 65 %, respectively (bottom). The corresponding improvement predicted from simulation of polished BGO crystals (Table 1) was 36, 41, and 98%, respectively. The relatively large discrepancy between simulated and measured values might be explained by (1) In the simulations, the crystal face in contact with the photodetector was always assumed to be polished. In the measurements, the crystal was pseudo-polished/semi-ground at best; (2) The calculation of the average light collection fraction from the simulation may have been weighted incorrectly with different points of light produc-

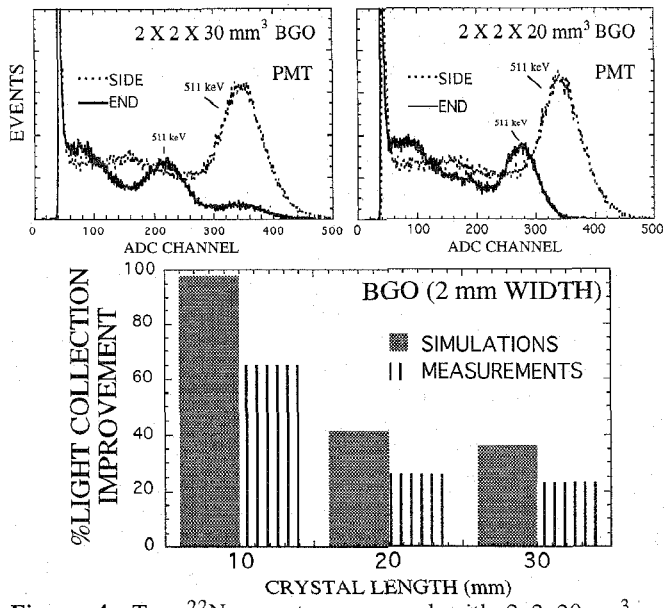

Figure 4. Top: ^{22}Na spectra measured with 2x2x20mm^3, and 2x2x30mm^3 BGO and PMT for side and end readout. See legends. Below: Comparison between simulations and measurements of light collection improvement of side over end readout.

tion (depth of interaction); and (3) The true reflection coefficient of white Teflon tape may be different than the 98% value assumed in the simulations. However, the point is that both simulations and measurements show side readout provides a large improvement in light collection efficiency over end readout, especially for longer and narrower crystals.

A crucial requirement for a PD readout for PET is that excellent coincident timing for annihilation gamma rays is possible. Figure 5 demonstrates that this condition is satisfied using ^{22}Na source irradiation and side readout. We used the LSO/PMT combination as the TAC Start and the LSO/PD as a Stop. The CFD thresholds were set to zero and the digitized TAC and energy values for each event were acquired in list mode. The top of Figure 5 shows the raw TAC spectrum with no energy thresholds applied. Noise contaminates the measured results. If we consider only those events contributing to the major peak (7.0 ns FWHM) in the raw TAC spectrum (shaded region) the corresponding PD and PMT energy spectra are shown in the middle two plots of Figure 5. We see that mostly PD noise and some photopeak events contribute to this major TAC peak without an energy threshold. Because of the high PD noise contribution without an energy threshold, all energies from the PMT contribute to the TAC spectrum, as seen in the middle, right of Figure 5. The same analysis applied to the far right peak in the raw TAC spectrum showed that it was caused mostly by the PD noise.

If we allow only those events that contribute to the 511 keV photopeak of the PD channel (small shaded region shown in the middle, left plot of Figure 5) the associated TAC and PMT spectra are shown in the bottom two plots of Figure 5. The timing resolution of this "gated" TAC peak is 9.4 ns FWHM (extracted from a fit to a Gaussian distribution). We do not yet understand the origin of the structure to the left of this gated TAC peak. Perhaps there is a significant LSO decay time component faster than the dominant 40 ns value in this particular crystal. As expected, by requiring that only 511 keV photopeak events in the PD contribute to the TAC measurement, only 511 keV photopeak events in the PMT are observed, as seen in the bottom right of Figure 5. An exact experiment was performed using ^{18}F as the source of 511 keV annihilation gamma rays. Identical results were obtained for the timing resolution.

As mentioned in Section IIIB, the sensitive area of the PD (3x3x30 mm^3) used for the energy and timing resolution measurements was much larger than required to read out either the 2x2x10 or 2.5x2.5x20 mm^3 LSO samples from the side. With a smaller, better matched PD area, the noise voltage, and, thus, pulse timing jitter would be reduced, which implies better coincidence timing resolution results.

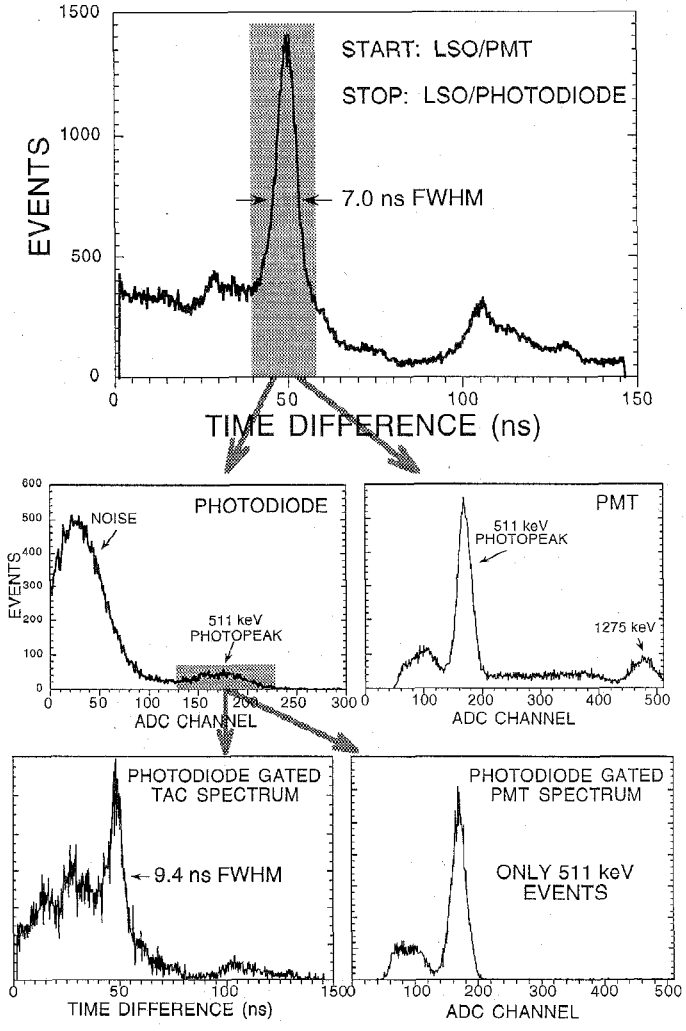

Figure 5. (Top) Measured "raw" coincident timing TAC spectrum with zero energy threshold for a ^{22}Na source. Start: 4x4x10mm^3 LSO crystal on a PMT. Stop: 2.5x2.5x20mm^3 LSO crystal on a photodiode. (Middle) Photodiode and PMT spectra corresponding to shaded region of top TAC spectrum. (Bottom) TAC and PMT spectra corresponding to photopeak region (shaded) of middle photodiode spectrum. A coincidence timing resolution of 9.4 ns FWHM was measured for this photodiode energy gated TAC spectrum.

IV. SUMMARY

We have proposed a feasible semiconductor photodetector readout scheme for PET scintillation crystal arrays using strips of silicon PIN photodiodes (PD) inserted in between crystal planes. The strips readout the crystals from the large side faces of the long and narrow crystals as opposed to the ends.

Because the photodetector planes are very thin no unusual dead area between crystals is introduced. The PD cannot be too thin because the device capacitance, and, therefore, noise increases with decreasing thickness. We have shown that with the side readout of the light, the fraction of the available scintillation light collected from 511 keV interactions is high (>90% for polished LSO) and roughly independent of the crystal length, width and surface treatments. This implies that extremely narrow crystals can be used, for higher detector resolution , if desired. In fact, both energy and timing resolution will improve as the PD area decreases due to a reduction in capacitive noise and dark current. However, in that case more channels are required to cover the same area. In addition, if the thickness of the PD becomes a significant fraction of the crystal width, the dead area fraction of the array increases. Although we described this new readout scheme for use in PET, it can be used for any discrete crystal array application.

With the conventional crystal end readout, the light collected is only a small fraction of that available and is highly dependent on crystal parameters. We have demonstrated comparable and, in some cases, better energy resolution characteristics with scintillation crystals coupled to a PD with side readout than with a PMT and the standard end readout. The boost in signal to noise ratio achieved with the side readout allows the LSO/PD combination to provide good coincident timing resolution. In principal, other types of reliable semiconductor photodetector devices that can be made thin enough to fit in between planes of scintillation crystal arrays can be used in this readout scheme (APDs, for example).

We note that the PD strips may be coupled one on one to the crystals rather than using a 1-D array of strips as shown in Figure 1. We also note that if depth of gamma ray interaction resolving power is desired for the array, each PD strip could, in principle, be segmented lengthwise. However, this requires more electronic channels for processing. Another possibility is segmenting each crystal in the array into two or more scintillators with different decay time characteristics coupled lengthwise. Pulse shape discrimination could be then used for a depth of interaction measurement, similar in principle to that reported previously [20]. This latter scheme poses no problems as long as the different scintillators used have sufficient light yield to be above the noise shoulder of the PD.

V. ACKNOWLEDGMENTS

This work was supported by grants from the Department of Energy (DE-CO3-87-ER60615), National Institutes of Health (R01-CA56655) and the State of California (IRB-0225). The authors gratefully acknowledge the valuable inputs from Dr. Lawrence MacDonald and Martin Tornai. We also thank Dr. Simon Cherry and Dr. Yiping Shao for their generous loan of electronics and LSO crystals.

VI. REFERENCES

[1] Moses, W.W.; Derenzo, S.E.; Geyer, A.B.; Huesman, R.H.; and others. The tuning algorithms used by the Donner 600 crystal tomograph. *IEEE Trans. Nucl. Sci.*, **36**-1:1025-9 (1989).

[2] M. Watanabe, H. Uchida, H. Okada et. al.. A High Resolution PET for Animal Studies. *IEEE Trans. Med. Imag* **11**: 577-80 (1992).

[3] S.R. Cherry, Y. Shao, S. Siegel et al. Optical Fiber Readout of Scintillator Arrays Using a Multi-Channel PMT: A High Resolution PET Detector for Animal Imaging. *IEEE Trans. Nucl. Sci.* **43-3**: 1932-7 (1996).

[4] M.E. Casey and R. Nutt. A Multi-crystal Two Dimensional BGO Detector System for Positron Emission Tomography. *IEEE Trans. Nucl. Sci.* NS-**33**: 460-3 (1986).

[5] M. Dahlbom and E.J. Hoffman. An evaluation of a Two-dimensional Array Detector for High Resolution PET. IEEE Trans. Med. Imag. **7**: 264-72 (1988).

[6] S.R. Cherry, M.P. Tornai, C.S. Levin et al., "A Comparison of PET Detector Modules Employing Rectangular and Round Photomultiplier Tubes. *IEEE Trans Nucl Sci*, NS-42: 1064-8 (1995).

[7] JB Barton, E.J. Hoffman, J.S. Iwanczyk, et. a. A High Resolution Detection System for Positron Emission Tomography. *IEEE Trans Nucl Sci* **NS-30**: 671-5, 1983.

[8] S.E. Derenzo, T.G. Budinger and T. Vuletich. High Resolution Positron Emission Tomography Using Narrow Bismuth Germanate Crystals and Individual Photosensors. *IEEE Trans Nucl Sci* NS-**30**:665-70 (1983).

[9] SE Derenzo. Gamma-ray Spectroscopy Using Small Cooled Bismuth Germanate Scintillators and Silicon Photodiodes. *Nucl Instr Meth* **219**: 117-22 (1984).

[10] M Dahlbom, M.A. Mandelkern, E.J. Hoffman, et. al. Hybrid Mercuric Iodide (HgI_2) -- Gadolinium Orthosilicate (GSO) Detector for PET. IEEE Trans Nucl Sci NS-32: 533-7 (1985).

[11] R. Lecomte, J. Cadorette, A. Jouan, et. al. High Resolution Positron Emission Tomography with a Prototype Camera Based on Solid State Detectors. *IEEE Trans. Nucl. Sci.* NS-37: 805-11 (1990).

[12] W.W. Moses, S.E. Derenzo, et. al. Performance of a PET Detector Module Utilizing an Array of Silicon Photodiodes to Identify the Crystal of Interaction. *IEEE Trans Nucl Sci* **40-4**:1036-40 (1993).

[13] N.H. Clinthorne. Are Hydrogenated Amorphous Silicon Arrays Usable for Tomographic Imaging? *IEEE Nucl Sci Symp and Med Im Conf Rec* **3**: 1692-6 (1993).

[14] C.J. Marriott, J.E. Cadorette, R. Lecomte et. al. High Resolution PET Imaging and Quantitation of Pharmaceutical Biodistributions in a Small Animal Using Avalanche Photodiode Detectors. *J Nucl Med* **35**:1390-7 (1994).

[15] W.W. Moses, S.E. Derenzo, et. al. A Room Temperature LSO/PIN photodiode PET Detector Module That Measures Depth of Interaction. *IEEE Trans Nucl Sci* 42-4:1085-9 (1995).

[16] M.J. Paulus, J.M. Rochelle, D.M. Binkley. Comparison of the Beveled-Edge and Reach-Through APD Structures for PET Applications. *IEEE Nucl Sci Symp and Med Im Conf Rec* **4**: 1864-8 (1994).

[17] C. Schmelz, S.M. Bradbury, I. Holl, E. Lorentz et. al. Feasibility Study of an Avalanche Photodiode Readout for a High Resolution PET with nsec timing resolution. *IEEE Trans Nucl Sci* **42-4**:1080-4 (1995).

[18] G.F. Knoll, T.F. Knoll, T.M. Henderson. Light Collection in Scintillating Detector Composites for Neutron Detection. *IEEE Trans Nucl Sci* **NS**-35-1: 872-5 (1988).

[19] M. Moszynksi, M. Kapusta, M. Mayhugh, D. Wolski, S.O. Flyckt. Absolute Light Output of Scintillators. Presented at this conference.

[20] L.R. MacDonald, M. Dahlbom and M. Paulus. Investigation of Using PET Block Detector Technology for SPECT Imaging. *J. Nucl. Med.* **37**(5), May 1995.